

CFD-BASED DESIGN AND OPTIMIZATION OF A CRYOGENIC PISTON VALVE FOR LIQUID  
HYDROGEN FLOW CONTROL

*Original*

CFD-BASED DESIGN AND OPTIMIZATION OF A CRYOGENIC PISTON VALVE FOR LIQUID HYDROGEN FLOW CONTROL / Safaei, A.; Dalla Vedova, M. D. L.; Maggiore, P.. - In: INTERNATIONAL JOURNAL OF MECHANICS AND CONTROL. - ISSN 1590-8844. - 26:2(2025), pp. 69-82. [10.69076/jomac.2025.0026]

*Availability:*

This version is available at: 11583/3009234 since: 2026-03-25T21:02:22Z

*Publisher:*

ASTRA M B S.r.l.

*Published*

DOI:10.69076/jomac.2025.0026

*Terms of use:*

This article is made available under terms and conditions as specified in the corresponding bibliographic description in the repository

*Publisher copyright*

(Article begins on next page)

# CFD-BASED DESIGN AND OPTIMIZATION OF A CRYOGENIC PISTON VALVE FOR LIQUID HYDROGEN FLOW CONTROL

Arash Safaei\* 

Matteo Davide Lorenzo Dalla Vedova\* 

Paolo Maggiore\* 

\* Department of Mechanics and Aerospace Engineering, Politecnico di Torino, Italy

## ABSTRACT

Thanks to their reliability and accuracy, piston valves are widely used in pressure regulation systems. This is especially true in the aerospace sector, where cryogenic fluids such as liquid hydrogen are commonly handled, making the design and operation of these valves particularly critical. However, the development of piston valve technology for cryogenic applications is still relatively limited, mainly because of the challenges involved in creating systems that can operate reliably in such harsh conditions. This highlights the need for more detailed studies and simulations using CFD tools and predictive models. To achieve efficient and stable performance of a piston pressure-regulating valve in a cryogenic environment, it is essential to understand both the strengths and the limitations of this technology under extreme thermal and mechanical loads. The work presented here focuses on a preliminary analysis and optimization of a piston valve operating with liquid hydrogen for pressure control purposes. Special attention is given to the dynamic behavior of the piston body, particularly regarding the robustness and controllability of its response. The study explores the motion of the piston in a low-viscosity flow, as well as the thermodynamic and fluid-dynamic characteristics of the valve system. Flow field simulations are carried out using CFD tools, and the results are combined with system response data obtained from a Simulink dynamic model. Finally, the outcomes are critically analysed to identify the regions where the valve is most affected by thermal and mechanical stresses, suggesting possible design improvements.

Keywords: aerospace systems, CFD analysis, cryogenic hydrogen, fluids, simplified fluid dynamic numerical models

## 1 INTRODUCTION

Piston valves are fundamental components in pressure regulation systems across various sectors, including aerospace, aeronautics, and energy. Their capacity to maintain accurate control over fluid pressure is particularly critical when dealing with cryogenic media such as liquid hydrogen, which exhibits extremely low temperatures and distinctive fluid-dynamic behaviour. Nonetheless, operating piston valves under such extreme conditions introduces several engineering challenges, primarily related to the handling and control of cryogenic fluids. Liquid hydrogen, widely employed as a propellant in aerospace propulsion systems, exhibits thermophysical properties that differ substantially from those of fluids at ambient temperature.

When gases are cooled to cryogenic levels, they condense into highly dense liquids, resulting in pronounced variations in parameters such as density, viscosity, and thermal expansion. These specific features constitute fluid dynamic challenges for pressure piston valves designed for fluids with more conventional properties. In addition, thermal contraction of valve components can affect tolerances and clearances, thereby compromising the functionality of the valve. Furthermore, liquid hydrogen has an exceedingly low viscosity compared to fluids at ambient temperature. This low-viscous fluid has the potential to influence the fluid's flow behavior within the valve, resulting in flow restrictions, pressure drops, and increased wear and strain on valve components. In such circumstances, maintaining precision pressure control becomes even more crucial. Cryogenic fluids have a natural tendency to boil and vaporize when exposed to higher temperatures. This can occur during the pressure reduction procedure or even when the flow reaches high velocities, resulting in phase changes within the valve itself. These phase changes can destabilize the flow control mechanisms and make it difficult to maintain precise pressure regulation.

---

Contact author: Arash Safaei<sup>1</sup>

<sup>1</sup> C.so Duca degli Abruzzi 24, 10129, Turin, Italy.  
E-mail: [arash.safaei@polito.it](mailto:arash.safaei@polito.it)

This study therefore concentrates on a preliminary CFD-based analysis and optimization of a piston valve operating with liquid hydrogen, aimed at addressing the complex fluid-dynamic phenomena associated with cryogenic conditions. A simplified dynamic model of the piston's response is subsequently developed for both the optimized and non-optimized configurations, allowing a comparative evaluation of the valve's regulating performance and overall efficiency. The analysis begins by creating a simplified geometry, suitable for the CFD analysis, of the main piston body of a generic pressure regulating valve. By simulating the behaviour of liquid hydrogen flow across the piston's body, it is then shown how the results of the performed CFD simulations provide a clear visualization of the critical aspects such as flow patterns, pressure distribution, velocity flow field and recirculating zones.

## 2 PROBLEM ANALYSIS AND OPTIMIZATION

The analysis and optimization of the simplified piston valve architecture (Fig. 1) carried out in this work are grounded in fundamental fluid-dynamic principles and in the physics governing flow through constricted passages. To optimize a conventional pressure-regulating valve for cryogenic applications, a thorough understanding of its individual components, along with their respective advantages and limitations, is essential. A pressure regulating valve can govern the fluid pressure of a feeding system using the mechanical forces acting on a control spring and the relative movement of the commanded piston. This is accomplished by adjusting the valve's opening to balance the forces operating on the piston itself, thereby maintaining a stable and controlled outlet port pressure. This kind of valve is commonly used in numerous industries to maintain the desired pressure levels in fluid systems. If the pressure at the outlet port fluctuates, owing to recirculation zones or chaotic velocity field downstream the control surfaces, the piston's position will start to change continuously to maintain the desired pressure. If the outlet pressure falls below the set pressure, the piston will move to allow more fluid to pass and increase the pressure. Instead, if the outlet pressure exceeds the specified pressure set value, the piston will move to restrict the flow and therefore to counterbalance this perturbation. The formation of flow recirculation regions and pronounced local pressure drops within a pressure-regulating valve represents a critical phenomenon, as it can strongly influence the system's thermal behaviour and dynamic stability, ultimately affecting the overall performance of the regulating mechanism. Complex fluid dynamics, valve geometry, and operational conditions frequently give rise to these two phenomena, which are closely related. Understanding the impact of these criticalities is essential for comprehending their potential effects on operating efficiency, safety, and valve's integrity. Fluid recirculation zones are regions within and around the valve where fluid flow reverses or becomes stagnant, instead of passing smoothly through the valve.

Such regions may develop due to several factors, including suboptimal valve geometry, unsuitable flow conditions, or specific fluid properties that promote turbulence and flow separation [1]. These effects can, in turn, generate localized heat transfer issues within the system. Fluids that are stagnant or move slowly can cause temperature stratification, leading to the freezing or overheating of valve components. These thermal variations can compromise the structural integrity and functionality of the valve and its surrounding components [2]. In addition, fluid recirculation zones frequently cause pressure fluctuations and instability downstream of the valve. As the fluid flow becomes erratic, pressure levels may fluctuate, influencing the valve's overall pressure regulation performance. These fluctuations may lead to pressure levels outside of the designed range, compromising the safety and reliability of the system. The stagnant or reversing flow can transport abrasive particles or contaminants that damage the valve's internal surfaces. This erosion may reduce the valve's efficiency and performance over time, necessitating maintenance and possible component replacement, particularly when dealing with cryogenic fluids such as liquid hydrogen. Large localized pressure drops can induce cavitation, which occurs when the fluid pressure falls below the vapor pressure, resulting in the formation and disintegration of vapor bubbles. This process of cavitation generates intense pressure waves and vibrations that can cause damage to the valve and adjacent components [3-4]. In addition, a significant localized pressure drop might interfere with the controllability of the valve. As unexpected pressure drops occur, the valve may struggle to maintain its desired pressure setpoint, resulting in system instability and fluctuations [5]. For the aforementioned reasons, it is crucial to develop valve architectures and mechanisms capable of minimizing the effects of these critical phenomena. As a starting point for the present analysis, a pressure drop of 23 bar is imposed across the entire system, with liquid hydrogen serving as the working fluid. The initial geometry of the piston valve, together with the specified boundary pressure drop and the no-slip wall condition, define and close the fluid-dynamic problem. Subsequently, the key parameters are evaluated, including the total force acting on the piston,  $F$ , as well as the pressure and velocity distributions along the piston body, obtained from the CFD analysis.

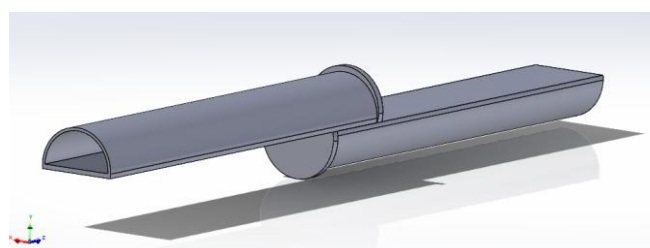


Figure 1 Three-dimensional representation of the simplified valve geometry.

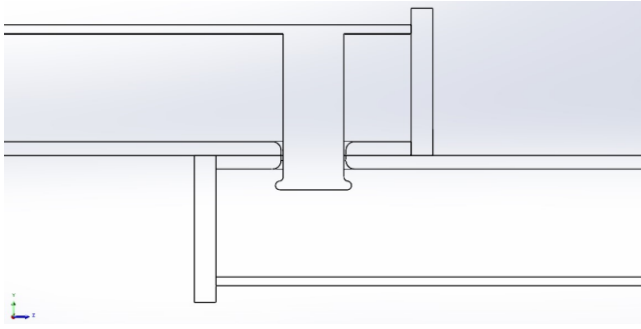


Figure 2 Cross section of the simplified valve geometry.

Determining the total force  $F$  acting on the piston body is a key step in evaluating the dynamic response of the system, particularly in terms of the position and velocity of the regulating mechanism. This force serves as input parameter for the Simulink-based dynamic model; therefore, its accurate estimation through CFD fluid-dynamic simulations is essential to ensure the reliability and precision of the modelling outcomes. Regarding the piston body, an effective aspect of the fluid-dynamic and mechanical optimization involves the thickness of its stem. A thicker piston stem provides the advantage of reducing the traction force exerted by the fluid flow, since the effective area of the annular surface on which the flow acts is smaller. Consequently, the piston experiences lower mechanical stress, which contributes to improved durability and operational lifespan. Moreover, having a thicker stem gives more inertia to the piston, and its robustness contribute to making it less sensitive to possible imbalance of forces with respect to a thinner and less inert piston. In addition, the distributed load of the flow along the stem, which causes a bending moment on the stem itself, causing it to deflect, is smaller if the resistant section of the stem is larger. For this reason, the proposed simplified architecture features a central piston body designed with a robust and carefully optimized geometry, allowing the cryogenic fluid to flow through it smoothly without encountering sharp edges or abrupt geometric variations. Such design considerations help prevent flow separation or the formation of recirculation zones near the crown orifice, which plays a key role in governing the pressure reduction process. Another optimization performed in this work on the valve design is the piston body passing through the conventional orifice which divides downstream from upstream, to create a circular crown-shaped zone for the passage of the flow (Fig. 3). This area shall be designed in such a way that the flow has a reduction of pressure equal to that set by design: in this way, if the piston regulating mechanism is to suffer a damage and therefore no longer work efficiently, the piston would still remain in axis providing the demanded area to reduce the upstream flow pressure to the desired value of downstream. This solution, properly implemented from an engineering point of view (i.e. by connecting the piston axis to a guide to maintain the axis straight), allows for a more robust and reliable pressure regulating mechanism, decoupling the pressure reduction function from that of regulation in case of system failures.

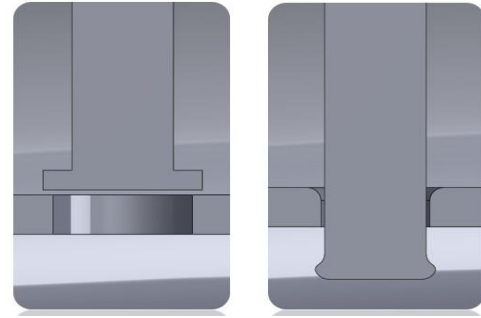


Figure 3 Comparison between the non-optimized piston body (left) and the optimized design (right).

As demonstrated by the CFD analysis results, the optimized piston configuration, which is featuring a body that passes through the circular crown orifice, experiences a lower overall force acting upon it, which is also significantly more stable over time compared to the total force observed in the conventional design, where the piston pushes directly toward the orifice (Fig. 3, left). A more constant force acting on the piston results in reduced oscillations during the pressure regulation phase, thereby improving the valve performance. Furthermore, if the total force acting on the piston is small enough, the piston inertia, combined with the action of the control spring and the viscous force of the flow, more effectively dampen the movement of the piston itself, reaching the desired equilibrium position with a contained number of oscillations compared to the non-optimized case.

## 2.1 NUMERICAL MODEL

In valve design, dedicated damping devices are seldom employed, as the combined influence of flow resistance and viscous effects inherently provides sufficient damping action [6]. For this reason, damping effect will not be considered as caused by a physical damper in the model, but from the viscous action of the liquid hydrogen flow. In the mathematical differential model of the problem, the effect of the downstream and upstream flow acting on the piston body is taken into consideration. To assess the performance of the valve, it is mandatory to calculate the time required for the piston to reach its equilibrium position, which is a function of the resultant total force  $F$ , input of the model. The characteristic time of the system is the time it takes for the piston to reach the equilibrium position required to achieve the set pressure reduction and maintain that value. Therefore, a pressure regulating valve with high performance is desired to respond quickly to a pressure perturbation while maintaining the shortest possible characteristic time. The simplified model of the optimized pressure-regulating valve can be idealized as a mass–spring–damper system, where the mass corresponds to the piston body, the damping effect arises from the viscous action of the flow passing through the valve, and the spring represents the mechanical element governing the piston position during the regulation phase. Consequently, the overall system can be described by a second-order differential equation of the classical form:

$$M\ddot{x} + C\dot{x} + Kx = F_{tot} \quad (1)$$

where  $M$  represents the mass of the piston,  $C$  the viscous coefficient,  $K$  the stiffness of the control spring, while the variable  $x$  represents the position of the piston under the action of the total force  $F_{tot}$ . It must be clearly considered that the displacement of the piston governs the relationship between the volume flow rate and the pressure drop across the valve, through the relation:

$$Q = C_d A \sqrt{\frac{2 \Delta p}{\rho}} = C_d 2\pi r x \sqrt{\frac{2 \Delta p}{\rho}} \quad (2)$$

where  $C_d$  is the discharge coefficient of the valve,  $r$  is the radius of the orifice,  $x$  is the displacement of the piston (which can be considered as the height of the geometrical cylinder which stands between the piston's plate and the orifice opening),  $\Delta p$  the pressure drop across the orifice and  $\rho$  the density of the fluid, in this case liquid hydrogen. The above equation shows how the maximum value of the volume flow rate  $Q$  is directly proportional to the displacement  $x$  the piston undergoes during the pressure regulation. This means that to each displacement  $x$  of the piston corresponds a maximum volume flow rate  $Q$  that can cross the circular crown orifice of the valve with a resulting drop of  $\Delta p$ . Therefore, if the downstream volume flow rate drops below the maximum value reported in Eq. (2), the downstream pressure will consequently rise, and this will cause the piston to move toward the closure of the valve, with a decrease in its displacement  $x$  as well as the flow passage area  $A$ . This displacement will directly lead to a further pressure decrease below the set value of  $\Delta p$ , hence regulating the pressure level as a function of the downstream flow condition of the valve. The objective of the implemented numerical model is therefore to compute the piston displacement  $x$  during the pressure regulation process, as obtained from the solution of the differential equation reported in Eq. (1). If the computed value  $x$  is consistent with the solution of Eq. (2), then the model will be able to forecast faithfully the physics of the system, allowing further assessments on the real dynamics of the valve's response starting from the theoretical implemented numerical model. To set properly the input total force  $F_{tot}$  in Eq. (1), a CFD analysis should be carried out, calculating the force contributions that act on the piston's body. These contributions can be then put into the model implemented on Simulink, which will simulate the dynamics of the system. For the complete definition of the dynamic model, the parameters of mass  $M$ , damping coefficient  $C$ , and spring stiffness  $K$  must be appropriately specified. Regarding the piston mass  $M$ , this parameter can be readily determined from the piston's geometry and material properties, which, in cryogenic environments, are typically selected from Inconel alloys or austenitic stainless steels [7-8]. The static model of the system gives the value of the stiffness  $K$ , by setting a starting suitable equilibrium position  $x_{eq}$  of the piston:

$$x_{eq} = \frac{F_{tot}}{K} \rightarrow K = \frac{F_{tot}}{x_{eq}} \quad (3)$$

The value of  $x_{eq}$  can be set equal to the piston's position in fully open valve's configuration, i.e., when the maximum volumetric flow passes through it. This position corresponds to the distance between the exit edge of the orifice and the bottom surface of the piston, value that can be estimated through Eq. (2) by setting the desired  $\Delta p$ , the required volume flow rate  $Q$  and the geometry of the orifice. The final parameter required to complete the dynamic model setup is the viscous coefficient  $C$ . Particular attention must be given to its accurate estimation, as the first-order differential term  $C\dot{x}$  plays a critical role in defining the damping behaviour of the system. The  $C$  coefficient binds the viscous force acting on the piston to the velocity of the piston itself, and it is dependent on the fluid dynamic properties. Given the very low viscosity of liquid hydrogen [9], the viscous action of the flow may be insufficient to dampen significantly the response of the piston, leading to a slow dynamic of the system with many oscillations until the equilibrium position is reached. Describing the mechanism of dissipation in a mathematical way is very difficult. The dampening effects are usually represented by idealized mathematical formulas. For many cases, these complex effects are adequately described by viscous equivalent damping. Therefore, the actual damping contribution of the liquid hydrogen flow, represented by the viscous coefficient  $C$ , can be accurately determined only through experimental measurements or CFD simulations, as it depends on inherently complex physical phenomena [10]. Analytically, this coefficient is computed as the ratio of the force acting on the piston and its related velocity. Since the only unknown value within the modeled system turns out to be the value of the viscous coefficient  $C$ , an initial guess value will be considered, moving preliminarily to a parameterized analysis. It is possible to calculate the critical value of the system, known the mass of the piston and the stiffness of the control spring (these values have been obtained through a prior lumped-parameter analysis here not reported), using the following formula:

$$C_{crit} = 2\sqrt{M * K} = 156.2 \left[ \frac{kg}{s} \right] \quad (4)$$

If the viscous coefficient  $C$  is below the critical value  $C_{crit}$ , then the system will be under-dampened, resulting in wide oscillations of the piston. The closer the value of the coefficient  $C$  to the critical one, the more important the fluid's dampening effect will be on the dynamics of the piston, which will reach the equilibrium position  $x_{eq}$  with gradually more contained oscillations. The Simulink-implemented model is schematically illustrated in Fig. 4. It is worth noting that a highly complex model is not required to perform a preliminary analysis of the piston dynamics within a liquid hydrogen flow. The main objective of this study is to provide a comparative assessment of valve performance and robustness between the optimized and non-optimized architectures, from both fluid-dynamic and dynamic perspectives.

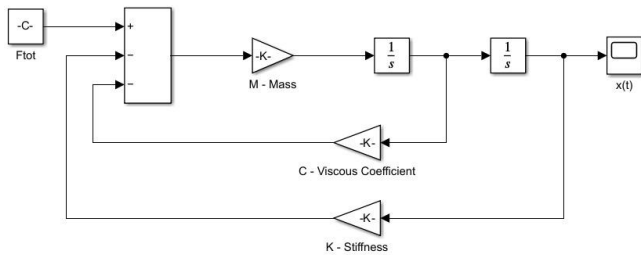


Figure 4 Schematic of the simplified Simulink model of the piston dynamics.

For the sake of this analysis, it is sufficient the computation of the coefficients of the differential model, together with the velocity and pressure field of the flow, in order to establish with accuracy, the total force  $F_{tot}$  acting on the piston of the valve and the contribution of the viscous effect of the liquid hydrogen carrying fluid, estimated directly through the CFD analysis. The complete dynamic model is solved in Simulink using sequential (waterfall) integrations, based on the differential equation derived from Eq. (1):

$$\frac{d^2x}{dt^2} = \frac{1}{M} (F_{tot} - C\dot{x} - Kx) \quad (5)$$

### 3 CFD SIMULATION

The CFD-driven optimization aims to refine the conventional piston valve design, enhancing its operational efficiency and reliability in managing low-viscosity fluids such as liquid hydrogen. This iterative process of analysis and optimization empowers the aerospace and cryogenic industries to develop piston valve designs that meet the stringent demands of cryogenic applications, ensuring safety, efficiency, and precise pressure control in extreme low-temperature environments. The purpose of the performed CFD's simulation is to provide an accurate and reliable fluid dynamic results in terms of velocity and pressure fields across the main body of the valve, in order to better understand and localize flow regions which may have a negative impact on the performance of the valve, in terms of localized high pressure drops, recirculating zones and high flow velocities. Particular attention must be given to the definition of the boundary layer, as accurately capturing the viscous effects along the wall is essential to ensure both convergence and fluid-dynamic accuracy of the simulations. Therefore, an adequate number of layers must be specified. To create a suitable and reliable mesh, it is necessary to ensure a good geometry's tessellation (as shown in Fig. 5), to approximate as much as possible the shape of the orifice to that of a circular crown rather than of a polygon. In this way it is possible to capture with high resolution the pressure and velocity field of the fluid in the proximity of the orifice small area avoiding singularities near sharp edges.

#### 3.1 GEOMETRY AND MESHING

A 3D cross-sectional model of the simplified main body of the valve is presented in Fig. 5. The CFD simulations were performed using SimScale, covering all stages from meshing to post-processing.

A patch-independent, tetra-dominant shell mesh was employed, together with tetra/mixed volume meshing based on the tetrahedral method. The volume mesh in the region surrounding the piston is illustrated in Fig. 7. To accurately capture the boundary layer, a prism mesh was applied along all wall surfaces. The smooth transition inflation method was adopted, with a growth ratio of 1.3 across 20 layers, as shown in Fig. 8. Mesh quality was assessed to verify element integrity and the absence of negative volumes. The minimum element quality was 0.03, with a maximum of 1.0, and an average quality of 0.88, for a total of approximately 9.7 million elements. The maximum precision of the model and its entities is  $5e-07$  m, which means that the mesh can capture the curvatures and small edges inside the geometry of the presented simplified design. Therefore, the mesh is suitable for the simulation.

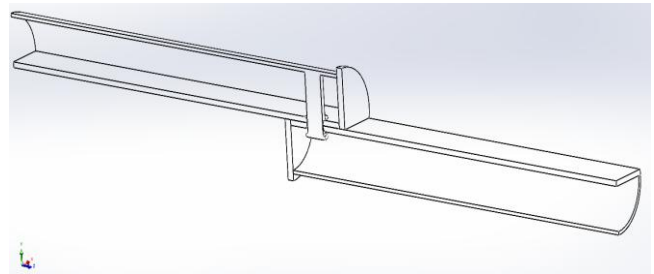


Figure 5 Cross section of the CAD model.

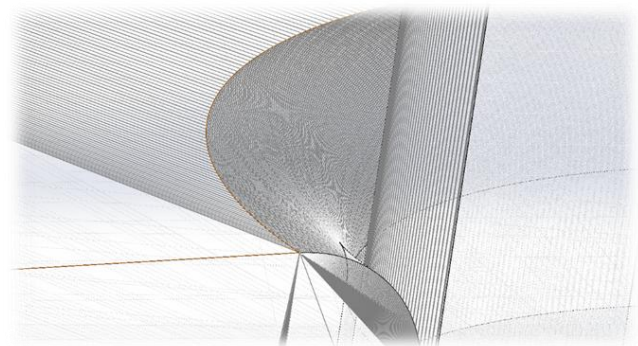


Figure 6 Tessellation of the piston body of the valve.



Figure 7 Volume Mesh with Tetrahedral cells.

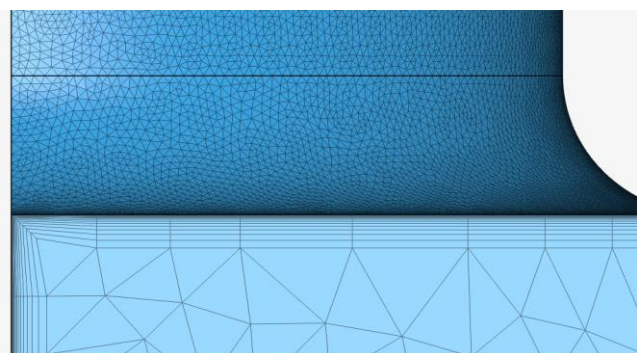


Figure 8 Boundary Layer inflation during meshing phase.

### 3.1 SOLVER SETTING

SimScale was used to solve the Reynolds-Averaged steady-state Navier–Stokes equations employing the  $k-\omega$  SST turbulence model under inviscid flow conditions. The wall boundaries were defined as no-slip, while pressure-driven boundary conditions were applied at the inlet and outlet. The selection of an appropriate turbulence model is crucial for achieving reliable simulation results. Among the most widely adopted approaches in CFD analysis are the  $k-\omega$  and  $k-\epsilon$  models. The main distinction between these two lies in their treatment of the viscous sublayer, with the  $k-\epsilon$  model providing a less accurate resolution compared to the  $k-\omega$  formulation [11]. Moreover, the  $k-\omega$  model is effective at resolving internal flows, separated flows and jets, flows with a high-pressure gradient, and internal flows through curved geometries [12] such as the orifice of the presented simplified valve. The realizable  $k-\epsilon$  model is an alternative that differs from the standard  $k-\epsilon$  model in two respects. Firstly, it contains a novel formulation for turbulent viscosity. The second difference is a new transport equation for the dissipation rate  $\epsilon$ , which is derived from an exact equation for the transport of the mean-square vorticity fluctuation. As a result, it mainly yields improved predictions for the spreading rate of jets, a superior ability to capture the mean flow of complex structures and for flows involving rotation, boundary layers under strong adverse pressure gradients, separation and recirculation. Both  $k-\epsilon$  and realizable  $k-\epsilon$  adopt wall functions. Therefore, regardless of which model is chosen for the simulation, the  $y^+$  values in the first cell near the wall must not be less than 30 or excessively greater than 100. If the mesh does not meet these criteria, the geometry must be meshed again to achieve reasonable results. Switching to a different turbulence model cannot compensate for a poor-quality mesh, especially when the selected model also relies on wall functions. The turbulent viscosity is calculated in a less complex manner in the standard  $k-\epsilon$  model, making it more stable. However, if the mesh captures the boundary sub-viscous layer appropriately, stability should not be an issue in either instance. Considering the respective advantages and limitations of the previously discussed models, the  $k-\omega$  SST turbulence model was ultimately selected for the simulations, as it effectively integrates the strengths of both the  $k-\omega$  and  $k-\epsilon$  formulations [13-14].

## 4 RESULTS AND DISCUSSION

All simulations met the convergence criterion within fewer than 1000 iterations, as illustrated in Fig. 9. The residuals of the computed solutions ranged between  $10^{-3}$  and  $10^{-5}$ , indicating that the CFD results can be regarded as practically steady, with only minor fluctuations. The figures that follow show the main differences between the optimized and non-optimized architecture of the piston: these significant differences are expressed in terms of pressure drop distribution of the fluid flow from the inlet to the outlet of the orifice, the local peaks of pressure, the flow's velocity field across the piston body as well as the main direction of the velocity vector, the recirculating zones and the instantaneous volume mesh rendering of the velocity particles motion across the piston. As far as concerns the interaction between the fluid flow with the smooth wall of the valve, the viscosity effect causes a decrease in the flow's velocity close to the walls, leading to the formation of the boundary layer shown in Fig. 14. The CFD simulations highlight the critical role of the geometric optimization performed on the piston body in shaping the fluid flow through the valve. The specific configuration of the piston and the surrounding circular crown orifice maintains the flow in a coherent, column-shaped jet, as illustrated in Figs. 12 and 16. This behaviour arises because the fluid is constrained to pass through the narrow yet elongated gap between the orifice wall and the piston stem, from the upstream to the downstream region. Consequently, this specific geometric arrangement promotes flow laminarization, preventing the pronounced pressure recovery typically observed downstream of a single orifice [15-19], and enabling a smooth and well-distributed pressure drop from the inlet to the outlet, as shown in Fig. 10. The non-optimized architecture is instead characterized by a huge localized pressure drop across the orifice, as can be noticed from Figs. 11, 13 and 15.

If the pressure drop is confined in a very small area, thus not having enough space to smoothly transition between a high pressure zone to a lower one, this will inevitably lead to a faster and more energetic turbulent flow, which translates into higher thermal exchange between the extremely cold liquid hydrogen flow with the wall and the piston itself. This will cause a continuous wear and thermal stress corrosion of the valve's regulating mechanism, causing the system failure during the valve's expected lifetime. Another significant difference between the optimized and non-optimized valve's architecture can be highlighted by comparing the pressure and viscous forces acting on the  $y$ -axis of the piston at equilibrium, which is the main axis along which the regulating mechanism acts. As can be clearly seen from Fig. 19 and 20, the non-optimized configuration involves a higher-pressure force with respect to the optimized one, and a lower viscous effect. This means that in the case of the non-optimized geometry, the piston must withstand a higher force ( $\bar{F}_{tot} = 190\text{ N}$ ), which is almost four times the average force that the optimized piston must deal with ( $\bar{F}_{tot} = 54\text{ N}$ ).

Therefore, an increase in the pressure force requires a more rigid control spring to maintain the piston's equilibrium position; consequently, the critical value  $C_{crit}$  of the system will increase, making it much more difficult for the liquid hydrogen flow to damp the piston's motion during the pressure regulation phase. Interpreting it in an alternative way, a greater force acting on the piston implies a greater amount of energy that must be dissipated over time, and since liquid hydrogen has a very low viscosity, the optimal solution would be to design the system so that the piston withstands a small total force, so as to have few oscillations and be able to dissipate the incoming energy from the flow over time. Furthermore, the time history of the pressure force in the case of the non-optimized piston, shown in Fig. 19, presents several large fluctuations around its average value, and this is due to the fact that the flow field under the piston surface is strongly irregular and chaotic, with the presence of vortices and recirculation zones that contribute to a continuous variation of the total acting force on the piston. The pressure regulating mechanism becomes clearly more complicated and less efficient, since the control spring is forced to work continuously to maintain the desired position of the piston. In the case of the optimized piston, however, it is noticeable from the plot reported in Fig. 19 that the time history of the pressure force is almost constant, with fluctuations much more contained than the non-optimized case, therefore representing a better and more effective piston dynamic response. Regarding the response time required for the piston to reach the desired equilibrium position, it can be seen from the plot reported in Figs. 21 and 22 how the optimized solution reaches the equilibrium position with a lower number of oscillations, about half of the oscillations performed by the non-optimized piston. These oscillations are clearly due to the low viscous effect of liquid hydrogen, which results in an extremely low viscous coefficient, below the critical value of the system  $C_{crit} = 156.2$ . Therefore, the optimized piston exploits fewer oscillations. Specifically, when considering a higher viscosity fluid like Oil SAE 120, the dynamic model implemented on Simulink confirms the validity of the analysis and optimization performed on the valve. It is evident that the optimized piston, when operating with high viscous fluids, displays a considerably reduced number of oscillations and a more significant damping effect compared to the non-optimized piston. The dynamic simulations performed in Simulink, solving the piston's differential model, reveal repeated oscillations that asymptotically approach a steady-state value. This behaviour occurs because the only damping contribution considered in the analysed system is the viscous action of liquid hydrogen, which alone is insufficient to fully attenuate the piston's motion. Furthermore, the piston mass is set to  $M = 0.038 \text{ kg}$  in the model simulation, so very little inertia opposes the motion of the piston, thus leading to continuous oscillations. As far as concerns the viscous  $C$  coefficient, it is computed through an iterative process starting from a guess value arbitrarily set equal to 10.

By taking the distribution of the piston's velocity from the solution of Eq. (1) implemented on Simulink, whose analytical behavior is shown in Fig. 21, and averaging over time this distribution in terms of amplitude of the velocity peak values [20], it is thus estimated the system's viscous coefficient, initially unknown. Combining the value of the total force acting along the piston axis in steady state configuration, obtained through CFD and shown in Fig. 20, and the average value of piston velocity, the following viscous coefficient is obtained:

$$C = \frac{F_{tot}}{\dot{x}_{piston}} = \frac{1.40 \text{ N}}{0.14 \text{ m/s}} = 10 \quad \left[ \frac{\text{kg}}{\text{s}} \right] \quad (6)$$

If this simple procedure is repeated iteratively, the convergence value of  $C = 4.75 \text{ [kg/s]}$  is obtained after four iterations with a residual error of 0.3 %, as shown in Table 1. This analytical procedure allows an estimation of the viscous coefficient based on the dynamics of the system. Nevertheless, in order to calculate a more reliable value of the viscous coefficient  $C$  of the real system, an experimental test is required, which is extremely expensive and complicated due to the fact that it would involve the measurement of the friction force between the piston's body and the walls of the valve (this friction contribution has been neglected for this preliminary study), as well as the piston's velocity caused by an applied force within liquid hydrogen environment, which is dangerous if not handled carefully within a dedicated experimental test bench.

Table I - Iterative computation of viscous coefficient  $C$

Iteration n°	$C$ [kg/s]	Error %
1	10.00	88.0
2	5.31	10.2
3	4.81	1.3
4	4.75	0.3
<b>Final value</b>	<b>4.75</b>	<b>0.3</b>

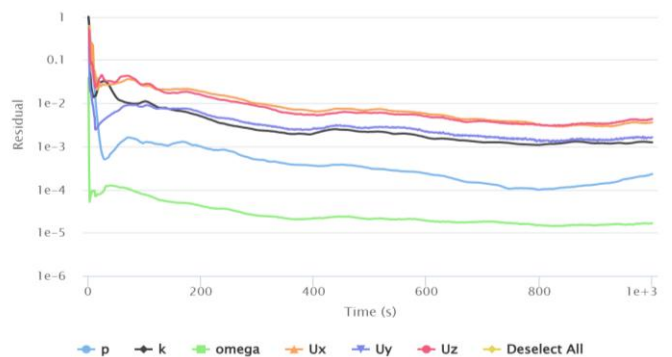


Figure 9 Residual convergence plot obtained from the simulation performed in SimScale.



Figure 10 Pressure field variation across the optimized piston body.

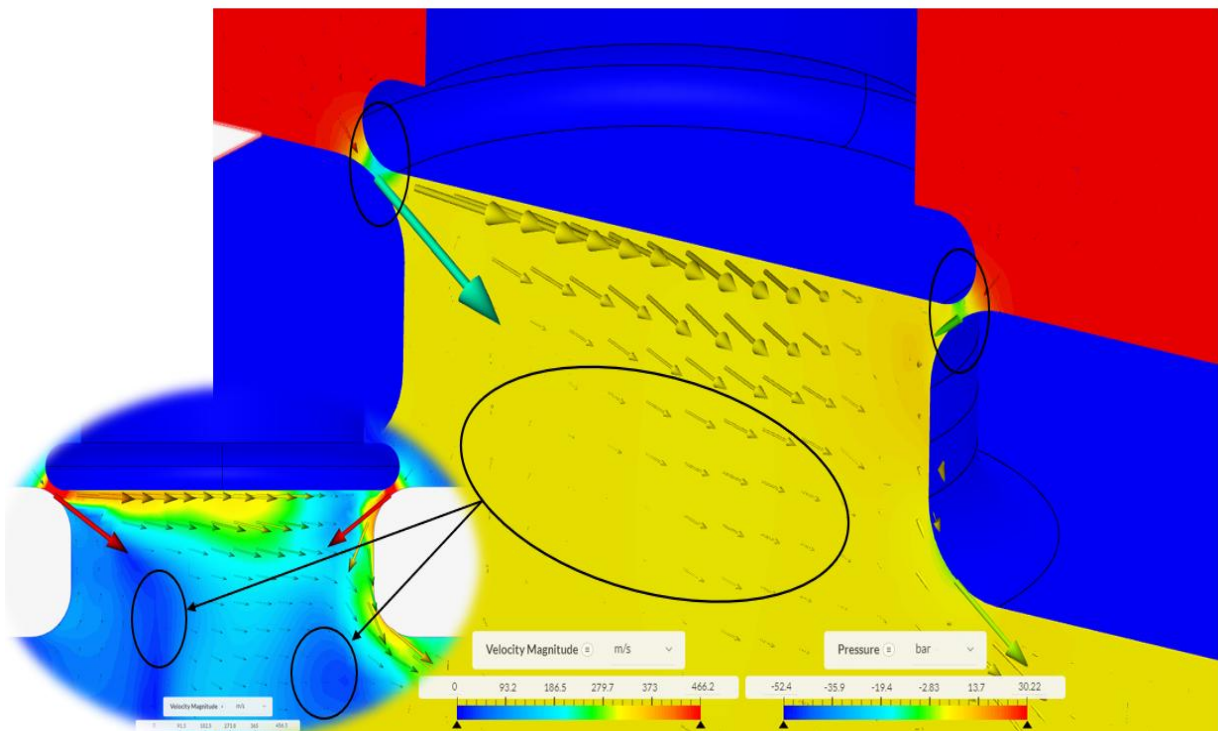


Figure 11 Pressure field variation across the non-optimized piston body. On the left the recirculation zones, on the top the localized pressure drops.

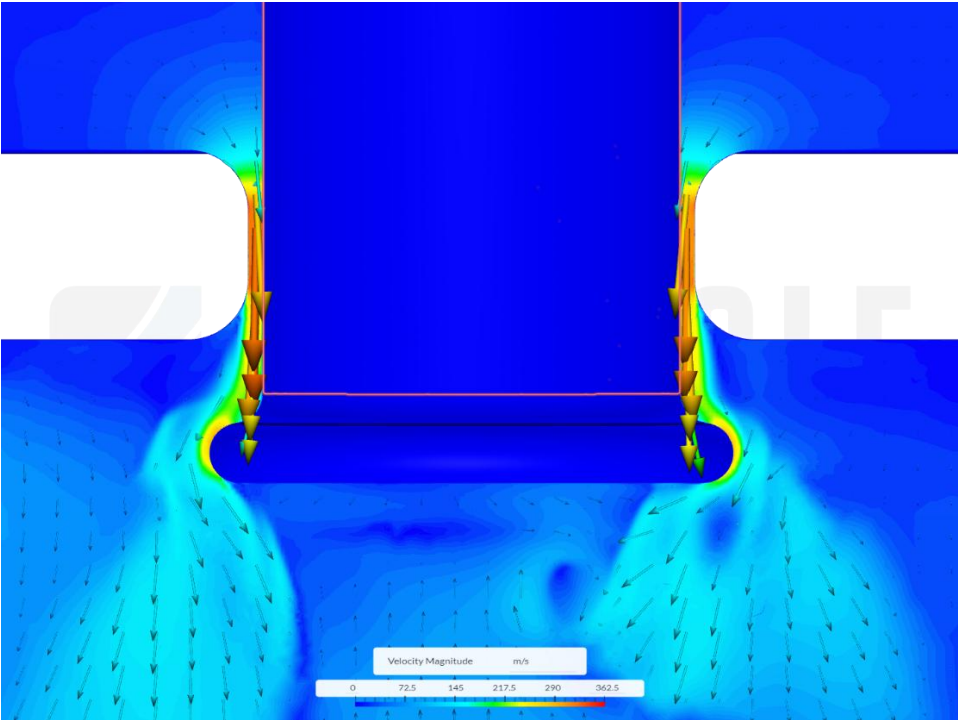


Figure 12 Computed velocity field of liquid hydrogen around the optimized piston body.

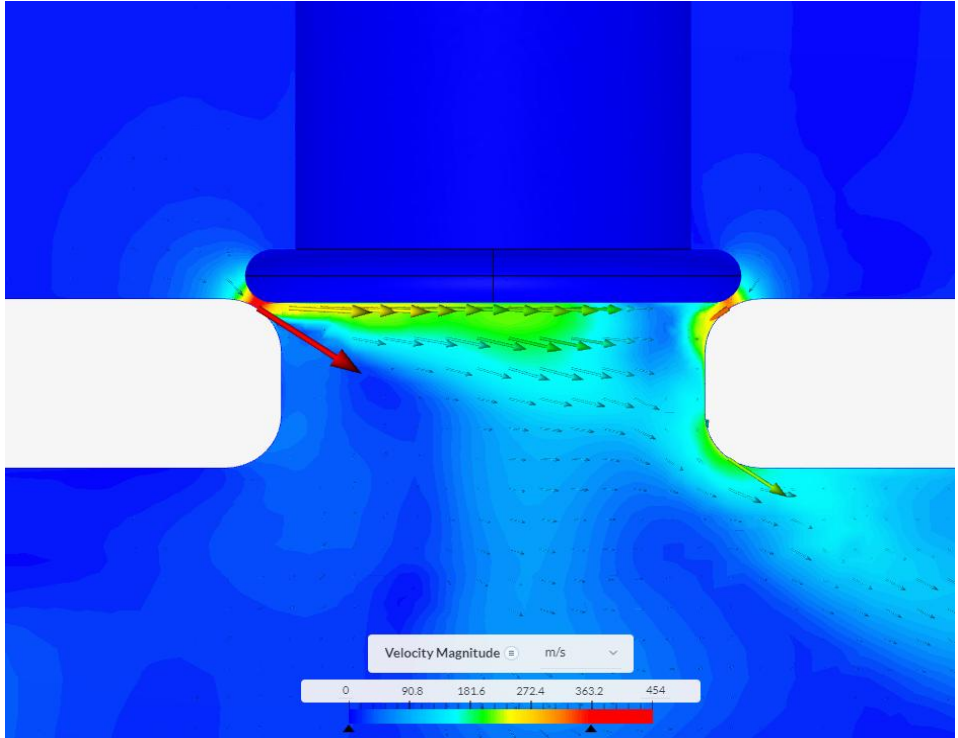


Figure 13 Velocity field of the LH2 flow around the non-optimized piston body.

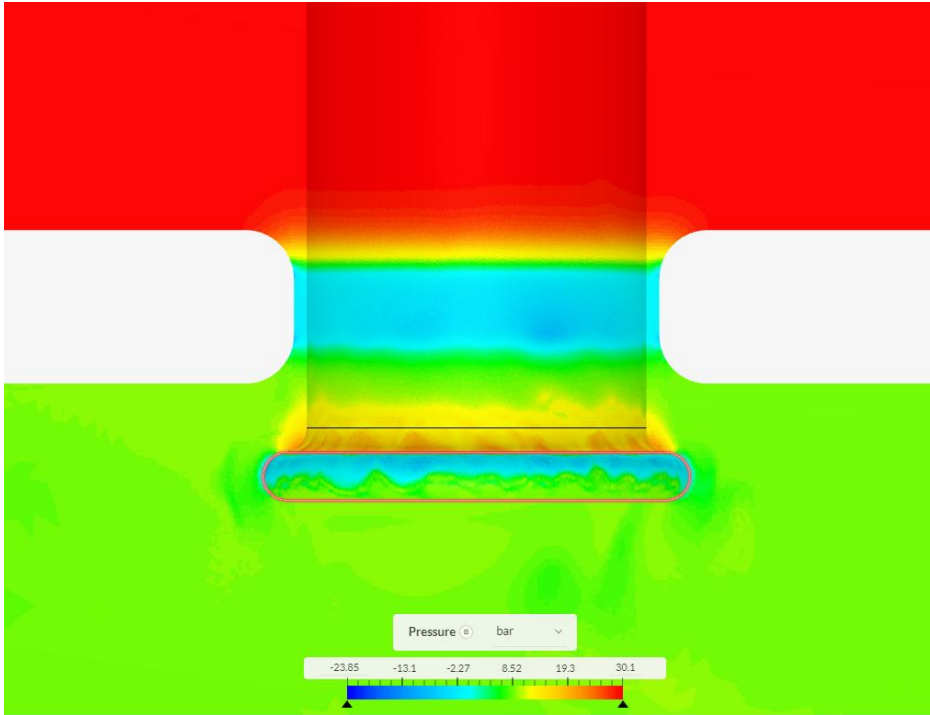


Figure 14 Pressure field of the LH2 flow around the optimized piston body.



Figure 15 Pressure field of the LH2 flow around the non-optimized piston body.

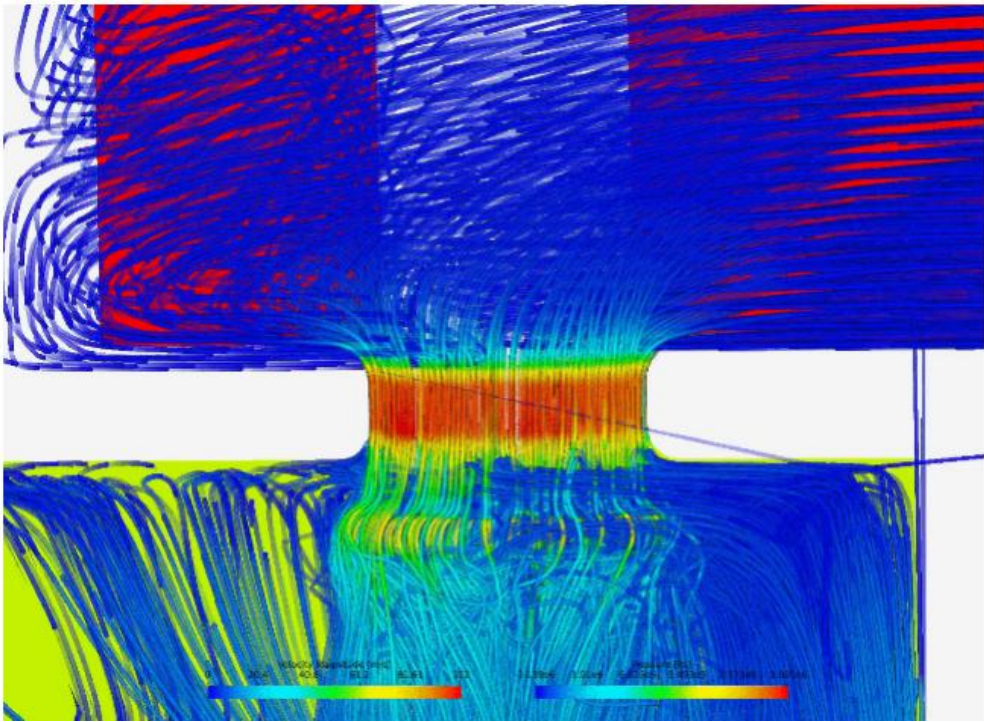


Figure 16 Laminarization of the flow jet across the optimized piston body of the valve.

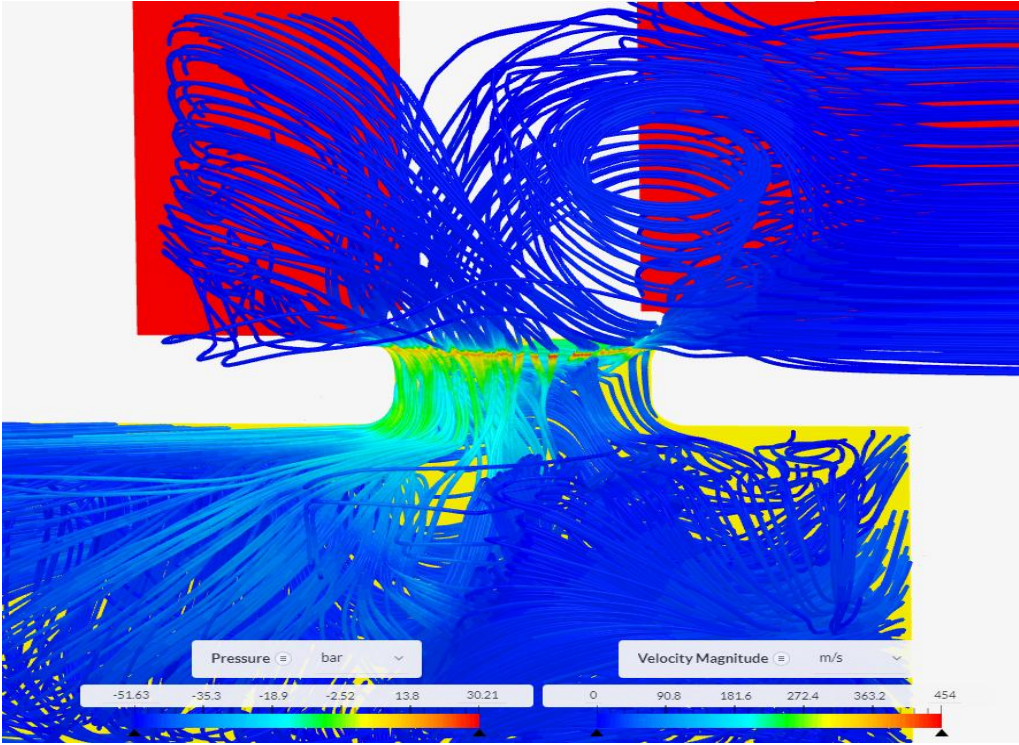


Figure 17 Laminarization of the flow jet across the non-optimized piston body of the valve.

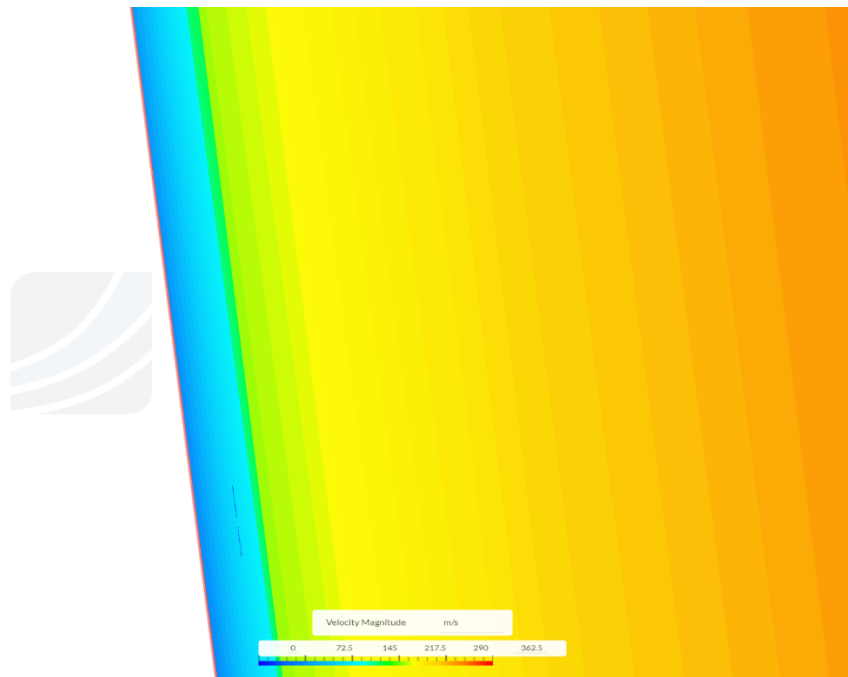


Figure 18 Boundary layer's capture in the proximity of the wall.

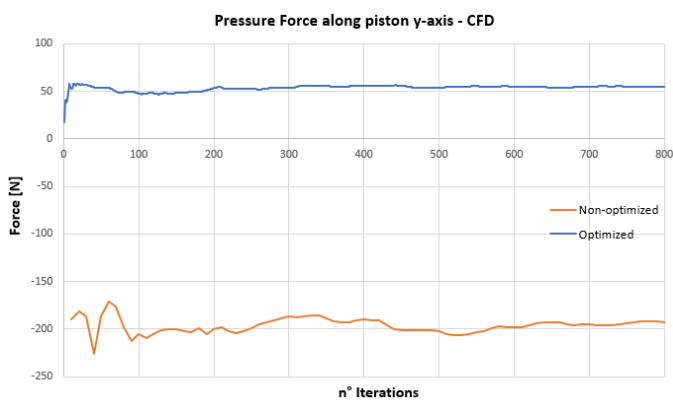


Figure 19 Pressure force along the y-axis of the piston body.

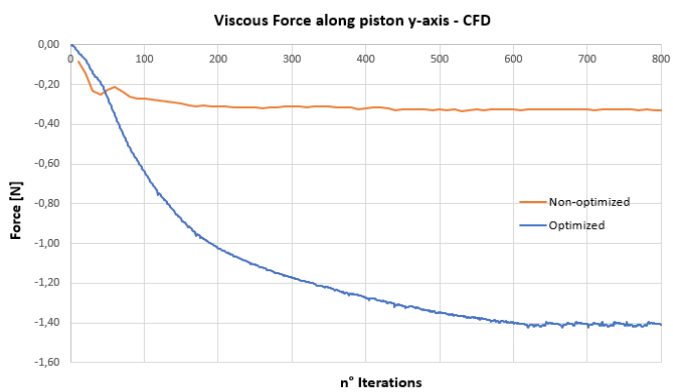


Figure 20 Viscous force along the y-axis of the piston body.

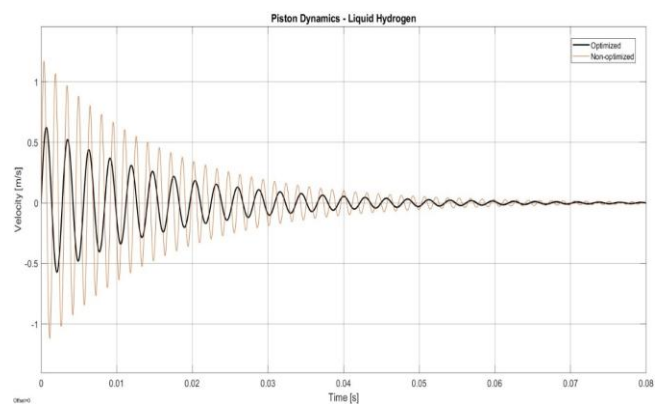


Figure 21 Comparison of the optimized and non-optimized piston dynamics with liquid hydrogen.

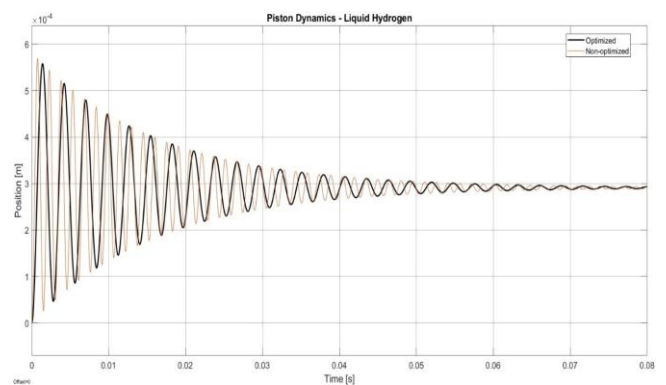


Figure 22 Comparison of the optimized and non-optimized piston dynamics with liquid hydrogen.

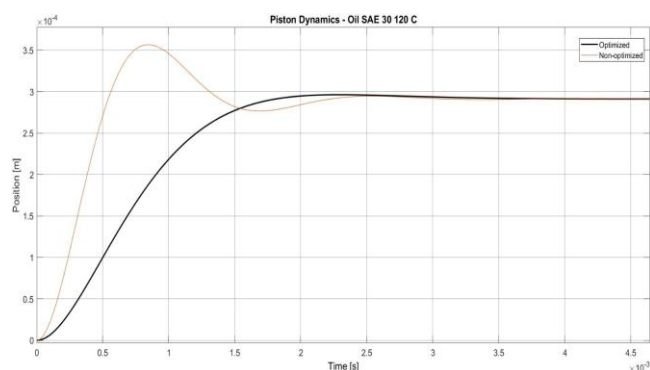


Figure 23 Comparison of the optimized and non-optimized piston motion with oil SAE 30.

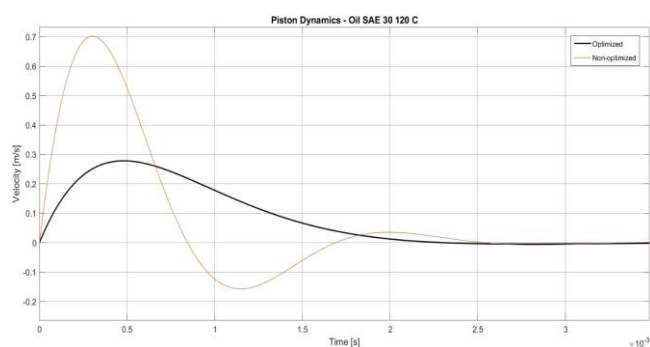


Figure 24 Comparison of the optimized and non-optimized piston motion with oil SAE 30.

## 5 CONCLUSIONS

A CFD-based preliminary study on a simplified liquid hydrogen pressure-regulating valve has demonstrated the benefits of geometric optimization in enhancing flow stability and valve performance. The optimized design reduces pressure losses and recirculation effects, while a simplified Simulink model successfully predicts the piston's dynamic response based on its geometry. The performed analysis and optimization via CFD are therefore able to assess and capture the main differences concerning the flow field between the presented architectures with good accuracy, thus validating the robustness and performance of the optimized piston's body. The proposed simplified pressure-regulating valve highlights the influence of liquid hydrogen flow on the piston's dynamic behaviour, particularly in terms of its position and velocity. Due to the extremely low viscosity of this cryogenic fluid, the system exhibits a lightly damped response with pronounced oscillations, which can be effectively controlled only through careful geometric and dynamic optimization. Moreover, the developed analysis framework can be readily extended to fluids with different viscosities and operating pressures, making the simplified valve concept a versatile solution for a wide range of fluid-dynamic applications. Future work will focus on manufacturing and testing the proposed optimized geometry in different fluid dynamic environments and pressure conditions, ranging from low to high-viscous fluids, to validate the real response of the piston with respect to the dynamic response of the numerical model.

## REFERENCES

- [1] Tabrizi A.S., Asadi M., Xie G., Lorenzini G. and Biserni C., Computational fluid-dynamics-based analysis of a ball valve performance in the presence of cavitation. *Journal of Engineering Thermophysics*, pp. 23, 27-38, February 2014.
- [2] Jin H., Zheng Z., Ou G., Zhang L., Rao J., Shu G. and Wang C., Failure Analysis of a high pressure differential regulating valve in coal liquefaction. *Engineering Failure Analysis*, Vol. 55, pp. 115-130, September 2015.
- [3] Niola V., Spirito M., Savino S. and Cosenza C., Vibrational analysis to detect cavitation phenomena in a directional spool valve. *International Journal of Mechanics and Control*, Vol. 22, No. 1, pp. 11-16, 2021.
- [4] Niola V., Savino S., Quaremba G., Cosenza C., Spirito M., Nicoletta A., Romagnuolo L. and Frosina E., Classification of different cavitation conditions in a proportional spool valve through vibrational analysis. *International Journal of Mechanics and Control*, Vol. 24, No. 1, pp. 53-60, 2023.
- [5] Wang Y. and Yang V., Central recirculation zones and instability waves in internal swirling flows with an annular entry. *Physics of Fluids*, Vol. 30, No. 1, January 2018.
- [6] Turgut S.S., *Wave Forces on Offshore Structures: Hydrodynamic Damping*. Cambridge University Press, pp. 265-284, July 2014.
- [7] Kendall E.G., *Metals and Alloys for Cryogenic Applications – A review*. Defense Documentation Center for Scientific and Technical Information, United States Air Force, January 1964.
- [8] MIL-HDBK-5J, *Metallic Materials and Elements for Aerospace Vehicle Structures*. Department of Defense Handbook, United States of America, January 2003.
- [9] Kim H.I., Han K.Y. and Park J.H., *Liquid Hydrogen Properties*. HANARO Utilization Technology Development Div, p. 32, 2004.
- [10] Lesieur G.A., *Damping in FE Models*. Encyclopedia of Vibration, pp. 321-327, 2001.
- [11] Minsheng Z., Decheng W. and Yangyang G., Comparative Study of Different Turbulence Models for Cavitation Flows around NACA0012 Hydrofoil. *Journal of Marine Science and Engineering*, MDPI, 2021.
- [12] Thakare H.R. and Parekh A.D., CFD analysis of energy separation of vortex tube employing different gases, turbulence models and discretisation schemes. *International Journal of Heat and Mass Transfer*, Vol. 78, pp. 360-370, November 2014.
- [13] Menter F.R., Zonal Two Equation  $k-\omega$  Turbulence Models for Aerodynamic Flows. *AIAA Paper*, No. 93-2906, 1993.
- [14] Menter F.R., Two-Equation Eddy-Viscosity Turbulence Models for Engineering Applications. *AIAA Journal*, Vol. 32, No 8, pp. 1598-1605, 1994.

- [15] Shivarudrappa K.B., Sargunar E.V.M. and Sakthivadivel R., An Experimental Investigation of Pressure Recovery Factor in Discharging Manifolds. *6<sup>th</sup> Australasian Hydraulics and Fluid Mechanics Conference*, Adelaide, Australia, 5-9 December 1977.
- [16] Dalla Vedova M.D.L. and Alimhillaj P., Study of new fluid dynamic nonlinear servovalve numerical models for aerospace applications. *Proceedings 2018 2nd European Conference on Electrical Engineering and Computer Science Eecs 2018*, pp. 483-490, 8910132, 2018.
- [17] Dalla Vedova M.D.L., Berri P.C., Corsi C. and Alimhillaj P., New synthetic fluid dynamic model for aerospace four-ways servovalve. *International Journal of Mechanics and Control*, Vol. 20, No. 2, pp. 105-112, 2019.
- [18] Dalla Vedova M.D.L. and Berri, P.C., A new simplified fluid dynamic model for digital twins of electrohydraulic servovalves. *Aircraft Engineering and Aerospace Technology*, Vol. 94, No. 1, pp. 79-88, 2022.
- [19] Poçari S., Alcani M., Alimhillaj P., Londo A. and Hoxha A., Numerical and experimental study of the pressure-compensated flow control valve in an hydraulic system using, mathematical model and LabVIEW. *International Journal of Mechanics and Control*, Vol. 25, No. 1, pp. 69-76, 2024.
- [20] Ponzo F.C. and DiTommaso R., *Valutazione della capacità dissipativa di un sistema strutturale*. Corso di Laurea Magistrale in Ingegneria Civile, Università degli Studi della Basilicata, 2011.